MAGNETOFLUIDIC BASED CONTROLLED DROPLET BREAKUP: EFFECT OF NON-UNIFORM FORCE FIELD: SUPPLEMENTARY MATERIALS

Sudip Shyam, Bhavesh Dhapola, Pranab Kumar Mondal*

Microfluidics and Microscale Transport Processes Laboratory,
Department of Mechanical Engineering,
Indian Institute of Technology Guwahati, Guwahati 781039, India
Email address for correspondence: mail2pranab@gmail.com; pranabm@iitg.ac.in

1. MAGNETIC FIELD DISTRIBUTION

In order to obtain the distribution of the external magnetic field in the flow domain, we perform a three-dimensional numerical simulation by using the finite element-based framework of COMSOL Multiphysics®. The governing equation describing the distribution of magnetic field is based on Maxwell's law, which for a static case (i.e., no current) can be written as (Griffiths 2017),

$$\boldsymbol{\nabla} \times \bar{\boldsymbol{H}} = 0 \tag{1}$$

$$\nabla \cdot \bar{\boldsymbol{B}} = 0 \tag{2}$$

where $\bar{\boldsymbol{H}}$, and $\bar{\boldsymbol{B}}$ is the magnetic field intensity, and the magnetic field flux density, respectively.

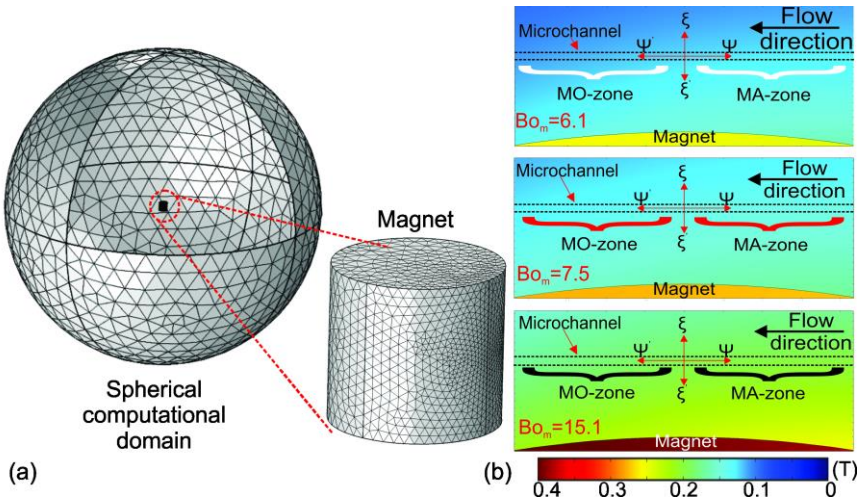

FIGURE 1. **(Color online)** (a) Typical meshing of the permanent magnet in the computational domain, (b) Distribution of the magnetic field along the peripheral direction in the left branch of the microchannel at "**MA**" and "**MO**" zone respectively. The flow direction is towards $\psi - \psi'$, while $\xi - \xi'$ indicates the direction away from the magnet.

Now, upon using the magnetic scalar potential V_m, the magnetic field intensity can be written as

$$\bar{\boldsymbol{H}} = -\nabla V_m \tag{3}$$

Employing the constitutive relationship $\bar{\boldsymbol{B}} = \mu_0(\bar{\boldsymbol{H}} + \bar{\boldsymbol{M}})$ where $\bar{\boldsymbol{M}}$ is the magnetization, the Eq. (2) can be rewritten as

$$-\boldsymbol{\nabla} \cdot (\mu_0 \nabla V_m - \mu_0 \bar{\boldsymbol{M}}) = 0 \tag{4}$$

Note that μ_0 in Eq. (4) is the permeability of the vacuum. The computation domain is such that it has a spherical outer air domain inside which the magnet is kept, as can be seen from Figure 1(a). While solving the above-mentioned equations Eq. (1)-(4), we use the normal component of the magnetic flux density $(\mathbf{n} \cdot \bar{\boldsymbol{B}} = 0)$ as zero (equivalent to magnetically insulating computational domain) at the boundary of the domain. The spherical outer domain (air domain) is kept sufficiently large such that the employed boundary condition has negligible influence on the vicinity of the field of the magnet. Free tetrahedral mesh of maximum element size of 2 mm, with a total of 2×10^6 elements were used in the present simulations, as can be observed from Figure 1(a). A stationary MUMPS solver with absolute tolerance of 10^{-6} was used for simulating the magnetic field.

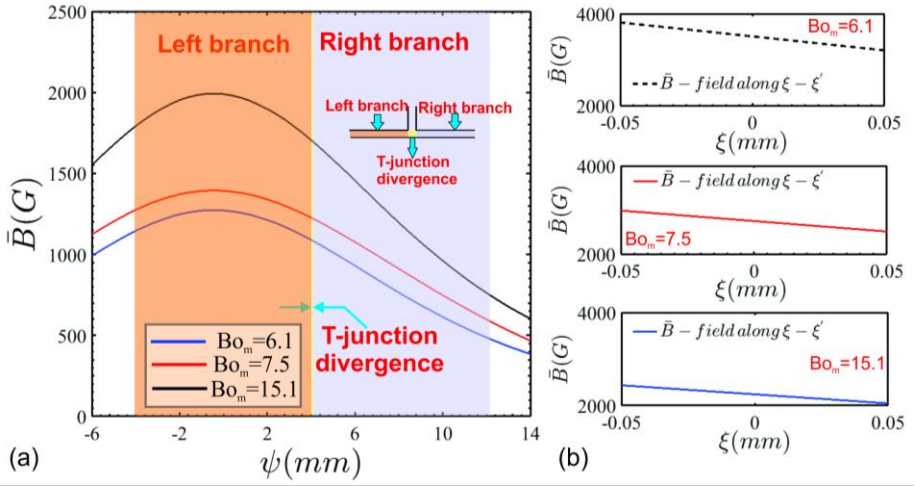

FIGURE 2. **(Color online)** (a) Variation of the magnetic flux density along the centerline for the channel in the left branch, T-junction divergence, and the right branch respectively. The orange, yellow and violet shaded region indicates the left branch, T junction and the right branch respectively. (b) Variation of the magnetic flux density $(\bar{B})$ along the $\xi - \xi'$ direction in the left branch of the T-junction divergence for the various cases under consideration.

In Figure 1(b), we show the distribution of the magnetic field flux density $(\bar{\boldsymbol{B}})$ along the left branch of the T-junction divergence for the various cases under consideration. The presence of the "MA (magnetically assisted) zone" in which the magnetic field supports the motion of the

ferrofluid droplet and the "MO (magnetically opposed) zone" in which the magnetic field resists the motion of the ferrofluid droplet is clearly marked in Figure 1(b).

We show in Figure 2(a) the magnetic field flux density ($\bar{\boldsymbol{B}}$) variation along the centerline of the channel in the left branch, T-junction divergence, and the right branch, respectively. As mentioned before, the magnetic field flux density is significantly more in the left branch of the LOC device in comparison to the right branch. We depict the variation of the magnetic field flux density ($\bar{\boldsymbol{B}}$) in the lateral direction of the left branch along the $\xi - \xi'$ in Figure 2(b). It can be clearly observed from Figure 2(b) that we encounter a significant drop in the applied force field gradient along the cross-section of the left branch (i.e., along $\xi - \xi'$ direction) for all the cases under investigation.

2. VALIDATION OF THE NUMERICAL FRAMEWORK

In this section, we discuss the benchmarking of the numerical framework adopted (to solve the droplet break up in presence of a magnetic field) with the experimental results. However, it may be mentioned here that the experimental scenario pertains to droplet train break up phenomena in the presence of a magnetic field, while the numerical experiments deals with the splitting of an isolated ferrofluid slug in the presence of a magnetic field. As already mentioned previously that these type of numerical strategy is adopted to save significant computational cost which may have incurred while simulating simultaneous generation and splitting of ferrofluid droplet train in a non-uniform magnetic forcing environment.

Thus, for an effective numerical validation, we fabricate another microfluidic channel of same characteristic dimensions as shown in Figure 3(inset). The prime intention of fabricating another microfluidic channel is to carryout experiments pertaining to isolate ferrofluid slug motion and its subsequent splitting in the presence of a non-unifrom magnetic field. As such this task permits to arrive at a qualitative validation of the proposed numerical modeling framework. Albiet the design of the microfluidic channel is similar to the one used in the experiments earlier, the only addition is the presence of another inlet through which additional continuour phase (Q_{c1}) can be injected as can be observed from inset of Figure 3. Injection of additional fluids enables us to control the gap between the individual mother droplet to several hundreds of micrometer (see

movie 5). When the gap between individual mother droplet is in the range of several hundreds of micrmeters, the droplet splitting can be approximated with an isolated droplet break-up scenario.

Figure 3 shows the morphological evolution of the neck of the droplet in the presence of magnetic field computed by using present numerical model and captured from our experiments. Important to mention here that the experimental results correspond to isolated droplet break-up scenario, created by using the new fabricated microchannel. A good qualitative match can be observed between numerical and experimental results. As already mentioned before that a droplet getting splitted following permanent obstruction, encounters three typical stages as discussed next. The initial stage is the sqeezing stage in which linear variation in the neck thinning is observed. This stage is followed by the transition stage where the evolution of the neck is predominantly exponential. The last stage is the pinch off stage, where the neck suddenly detaches and leading to the formation of two sister droplet. All these stages, as mentioned above, can easily be observed in both the numerical and experimental results demonstrated in Figure 3. This benchmarking endevour vouches for the reliability of our numerical approach in capturing the desired flow physics of interst.

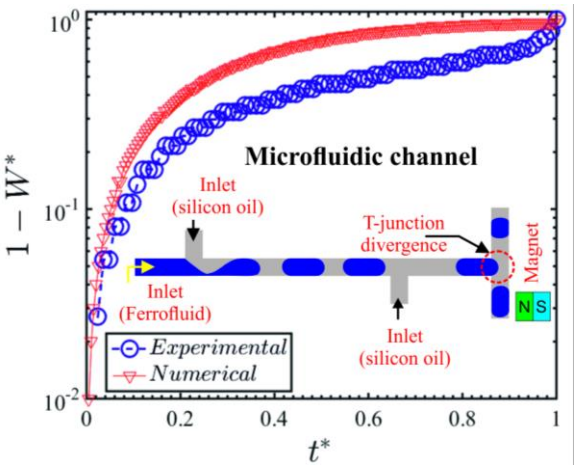

FIGURE 3. **(Color online)** Plot compares the thinning rate of the ferrofluid droplet in the presence of a magnetic field between the experimental and the numerical results. $W^* = w(t)/l$, where $w(t)$ and l denotes the instantaneous width of the droplet and the width of the microchannel. $t^* = t/t_0$, where t_0 is the droplet splitting time. $Bo_m = 6.1$. The inset shows the microfluidic channel fabricated to approximate an isolated droplet break-up scenario. Additional continuous phase is injected to control the gap between the mother droplet.

REFERENCES

Griffiths, D. J. (2017). *Introduction to Electrodynamics*. *Introduction to Electrodynamics*, Cambridge University Press. doi:10.1017/9781108333511